



Microglia contribute to the glia limitans around arteries, capillaries and veins under physiological conditions, in a model of neuroinflammation and in human brain tissue

Emely Joost¹ · Marta J. C. Jordão^{2,3} · Bianca Mages¹ · Marco Prinz^{2,4} · Ingo Bechmann¹ · Martin Krueger¹

Received: 17 September 2018 / Accepted: 12 January 2019 / Published online: 31 January 2019
© Springer-Verlag GmbH Germany, part of Springer Nature 2019

Abstract

Microglia represent resident immune cells of the central nervous system (CNS), which have been shown to be involved in the pathophysiology of practically every neuropathology. As microglia were described to participate in the formation of the astroglial glia limitans around CNS vessels, they are part of the neurovascular unit (NVU). Since the NVU is a highly specialized structure, being functionally and morphologically adapted to differing demands in the arterial, capillary, and venous segments, the present study was aimed to systematically investigate the microglial contribution to the glia limitans along the vascular tree. Thereby, the microglial participation in the glia limitans was demonstrated for arteries, capillaries, and veins by immunoelectron microscopy in wild-type mice. Furthermore, analysis by confocal laser scanning microscopy revealed the highest density of microglial endfeet contacting the glial basement membrane around capillaries, with significantly lower densities around arteries and veins. Importantly, this pattern appeared to be unaltered in the setting of experimental autoimmune encephalomyelitis (EAE) in CX3CR1^{CreERT2}:R26-Tomato reporter mice, although perivascular infiltrates of blood-borne leukocytes predominantly occur at the level of post-capillary venules. However, EAE animals exhibited significantly increased contact sizes of individual microglial endfeet around arteries and veins. Noteworthy, under EAE conditions, the upregulation of MHC-II was not limited to microglia of the glia limitans of veins showing infiltrates of leukocytes, but also appeared at the capillary level. As a microglial contribution to the glia limitans was also observed in human brain tissue, these findings may help characterizing microglial alterations within the NVU in various neuropathologies.

Keywords Microglia · Glia limitans · Basement membrane · Neurovascular unit

Ingo Bechmann and Martin Krueger these authors equally contributed

Electronic supplementary material The online version of this article (<https://doi.org/10.1007/s00429-019-01834-8>) contains supplementary material, which is available to authorized users.

✉ Ingo Bechmann
ingo.bechmann@medizin.uni-leipzig.de

✉ Martin Krueger
martin.krueger@medizin.uni-leipzig.de

¹ Institute of Anatomy, Leipzig University, Liebigstraße 13, 04103 Leipzig, Germany

² Institute of Neuropathology, University of Freiburg, Breisacher Straße 64, 79106 Freiburg, Germany

³ Faculty of Biology, University of Freiburg, Freiburg, Germany

⁴ BIOS Centre for Biological Signalling Studies, University of Freiburg, Freiburg, Germany

Introduction

Microglia represent the resident immune cells of the CNS (Kierdorf and Prinz 2017) with numerous functions under physiological and pathological conditions (Wolf et al. 2017). Among the different populations, microglia have been shown to contribute to 12–16% of cells within the CNS (Lawson et al. 1990; Mittelbronn et al. 2001). Since microglia as well as perivascular, meningeal, and choroid plexus macrophages are regarded as myeloid cells, they were initially believed to be of mesodermal origin. However, according to the currently accepted view, microglia are believed to predominantly derive from early yolk sac precursors (Alliot et al. 1999; Ginhoux et al. 2010; Kierdorf et al. 2013), which was also recently demonstrated for the non-parenchymal macrophages residing at the brain interfaces (Goldmann et al. 2016). Although a turnover of the microglial pool is potentially possible under defined conditions (Bechmann et al.

2005; Mildner et al. 2007), the contribution of blood-borne monocytes to the microglial pool proved only temporary, whereas the majority of microglia is regarded as a stable and self-renewing population throughout life (Ajami et al. 2007; Askew et al. 2017; Tay et al. 2017). With increasing age other glial cells as well as neurons rather decrease in number, while the relative numbers of microglia are shown to increase due to their capacity of self-renewal (Poliani et al. 2015; Tremblay et al. 2012). However, aged microglia undergo changes with respect to their morphology and function (Hefendehl et al. 2014; Sierra et al. 2007). Thereby, impaired microglial function or ‘senescence’ is characterized by a cellular dystrophy and partial fragmentation as indicated by an inhomogeneous cytoplasmic distribution of the microglia marker Iba-1 (Streit et al. 2009; Tischer et al. 2016).

Microglia are reported to play crucial roles in virtually every neuropathology including prion diseases, Alzheimer disease (AD), Parkinson disease, amyotrophic lateral sclerosis, or multiple sclerosis (Colonna and Butovsky 2017; O’Loughlin et al. 2018). Therefore, studying microglia under physiological and pathological conditions is mandatory for the development of respective treatment strategies. However, over the last decades, this research was inflicted by the lack of a specific microglia marker, which would allow differentiation of microglia from other brain macrophages or blood-derived myeloid cells under inflammatory conditions. Despite the broad spectrum of established microglial markers such as isolectin-B4, Iba-1, CD11b, CD68, none of them allows a clear-cut differentiation of microglia and meningeal or perivascular macrophages (Mildner et al. 2017). Even the widely applied mouse model genetically targeting the fractalkine receptor CX3CR1 with the green fluorescent protein (GFP) does not allow a discrimination of the different brain macrophages. Instead, it rather uniformly labels microglia in line with perivascular, meningeal, or choroid plexus macrophages as well as peripheral macrophages and monocytes (Jung et al. 2000; Wieghofer et al. 2015). However, recently, the transmembrane protein 119 (TMEM 119) and the P2Y₁₂ receptor were identified to discriminate between microglia and the other brain macrophages (Bennett et al. 2016; Mildner et al. 2017).

Although the term microglia is commonly used as the plural form, microglia do not represent a uniform, but a heterogeneous population (Gertig and Hanisch 2014). This heterogeneity is not only reflected by different functions, but also by differing immune phenotypes (M1 vs. M2) as well as differing expression patterns of diverse proteins such as MHC-II or co-stimulatory molecules (Gertig and Hanisch 2014). In this context, our group demonstrated the presence of a distinct subpopulation of microglia which shares certain features of dendritic cells. This subpopulation is characterized by the expression of the complement receptor marker CD11c under

control conditions and is further capable to express MHC-II (Prodinger et al. 2011; Immig et al. 2015). Of note, these cells were not only described to reside in predilection areas of multiple sclerosis but also to participate in the formation of the perivascular glia limitans (Prodinger et al. 2011). This structure is predominantly constituted by astrocytic endfeet and the adjacent astroglial basement membrane, which delineates the CNS parenchyma from the vascular compartment. Here, the contact of astrocytes with cerebral vessels not only orchestrates the development and maintenance of blood–brain barrier function (Zhao et al. 2015), but it also provides a crucial check point for extravasating leukocytes in the setting of neuroinflammation (Bechmann et al. 2007).

Although the perivascular glia limitans is primarily established by astrocytic endfeet, a participation of microglial endfeet has already been described more than 25 years ago (Lassmann et al. 1991). However, this intimate contact to the NVU has recently turned into focus again as microglia have been shown to promote vascular permeability and to be even involved in the phagocytosis of ischemic endothelial cells (Jolivel et al. 2015, Su et al. 2017). Furthermore, a microglial participation in the perivascular glia limitans (subsequently addressed as glia limitans) supports the view of microglial cells as possible gatekeepers for leukocytes to enter the neuropil upon extravasation under inflammatory conditions (Engelhardt et al. 2016). However, the cellular and molecular composition of the NVU including the presence of perivascular spaces is known to differ in arterial, capillary, and venous segments of the cerebral vasculature, thereby impacting on leukocyte recruitment (Dyrna et al. 2013; Sixt et al. 2001; Wu et al. 2009; Yousif et al. 2013). In this context, the question remains, whether the microglial contribution to the glia limitans is limited to post-capillary venules as sites of preferred leukocyte entry, or rather represents a universal feature of each segment of the vascular tree. Therefore, the present study is aimed to investigate and characterize the microglial contribution to the perivascular glia limitans in the arterial, capillary, and venous segments of the vascular tree. For this purpose, the analyses comprised immunoelectron microscopy and confocal laser scanning microscopy in CX3CR1^{+GFP} mice (Jung et al. 2000) under physiological conditions, as well as human post-mortem brain tissue. Furthermore, the participation of microglial endfeet in the formation of the glia limitans was addressed using CX3CR1^{CreERT2}:R26-Tomato reporter mice in chronic and acute stages of EAE.

Materials and methods

Experimental setup

All experiments involving animals were performed along the ARRIVE guidelines and according to the European Union

Directive 2010/63/EU. The animals used for our experiments were kept under pathogen-free conditions with free access to food and water. For electron microscopy, brain tissue obtained from five wild-type C57Bl/6 mice were used, whereas fluorescence microscopy analyses comprised tissue obtained from 6 CX3CR1^{+/GFP} mice (Jung et al. 2000) to analyse the contribution of microglial endfeet to the perivascular glia limitans under physiological conditions. To characterize the participation of microglia in the formation of the glia limitans in the setting of neuroinflammation, we applied the model of EAE in CX3CR1^{CreERT2}:R26-Tomato mice to differentiate resident microglia from blood-borne macrophages. Thereby, the analyses comprised spinal cord tissue obtained from the chronic phase ($n=5$), the acute phase ($n=6$) and non-immunized controls ($n=3$). Human post-mortem brain tissue was obtained from a body donor without evidence of any neurodegenerative diseases from the Institute of Anatomy at Leipzig University after institutional approval for the use of post-mortem tissues from the Institute of Anatomy at Leipzig University and in line with the Saxonian Death and Funeral Act of 1994, third section, paragraph 18, item 8. All authors declare that all experiments have been conducted according to the principles of the Declaration of Helsinki.

EAE induction in CX3CR1^{CreERT2}:R26-Tomato mice

In CX3CR1^{CreERT2}:R26-Tomato mice, EAE was induced as previously described (Goldmann et al. 2013, 2016). In brief, mice were subcutaneously immunized with 200 μ g of MOG_{35–55} peptide in Freund's complete adjuvant containing 1 mg of Mycobacterium tuberculosis (H37RA; Difco Laboratories, Detroit, Michigan, USA). Furthermore, mice received 250 ng of pertussis toxin via an intraperitoneal injection at the time of immunization and 48 h later. Mice were then subsequently analysed in the acute phase (score 3, typically between 15 and 17 days post immunization) and in the chronic phase (day 30 post immunization) of EAE.

Mouse tissue

CX3CR1^{+/GFP} mice ($n=6$) were transcardially perfused with saline followed by a fixative containing 4% paraformaldehyde (PFA, Serva, Heidelberg, Germany) in phosphate-buffered saline (PBS). Brains were carefully removed and allowed to postfix overnight in the same fixative. Serial sections of 50 μ m thickness were prepared using a vibrating microtome (Leica Microsystems, Wetzlar, Germany). Until use, the sections were stored in PBS containing sodium azide at 4 °C.

EAE spinal cord tissue of CX3CR1^{CreERT2}:R26-Tomato mice was fixed in 4% PFA (Serva) followed by cryoprotection in 30% sucrose with subsequent freezing and

preparation of cryostat sections. Until use, cryostat sections were stored at -20 °C.

Human brain tissue

Human post-mortem brain tissue was immersion-fixed in 4% PFA (Serva) formaldehyde-fixed, dehydrated, and embedded into paraffin. Paraffin sections were obtained on a microtome (Leica Microsystems). Sections were then deparaffinized in xylol and stepwise rehydrated in graded alcohol. Prior to immunofluorescence labeling, antigen retrieval was applied in citrate buffer (pH 6) at 96 °C for 10 min.

Fluorescence microscopy

For fluorescence microscopy, formaldehyde-fixed mouse brain and spinal cord sections were blocked with 5% normal goat serum (NGS) or bovine serum albumin (BSA), respectively, and 0,5% Triton X-100 (Roth, Karlsruhe, Germany) in PBS. To demark blood vessels and their surrounding basement membranes, primary antibodies for laminin (rabbit anti-laminin, 1:200; Millipore, Temecula, California, USA; AB19012) or collagen-IV (goat anti collagen-IV, 1:200; Millipore, AB769) were applied, whereas alpha smooth muscle actin (α -SMA, mouse anti α -SMA, 1:200; Dako, Glostrup, Denmark; M0851) was used to demark vascular smooth muscle cells of arterial vessels. Microglia were identified using antibodies directed against Tmem119 (rabbit anti TMEM119, 1:200, Abcam, Cambridge, UK), P2RY12 (rabbit anti P2RY12, 1:200, Sigma, Taufkirchen, Germany) or Iba-1 (rabbit anti Iba-1, 1:200; Wako, Osaka, Japan; 01919741), while MHC-II expression was addressed using a rat anti MHC-II antibody (1:200, Biolegend, San Diego, USA, 107602). Immunolabeling of CD11c-expressing microglia (rabbit anti CD11c, 1:100, Synaptic Systems, Göttingen, Germany) was performed in each of the applied reporter mouse models. Primary antibodies were allowed to incubate on the sections over night at 4 °C. After thorough rinsing, appropriate fluorochrome (AlexaFluor 488, AlexaFluor 568 or AlexaFluor 647) secondary antibodies (1:250, Life technologies, Eugene, OR, USA) were applied for 90 min at room temperature followed by thorough rinsing and counterstaining of nuclei with 4',6-diamidino-2-phenylindole dihydrochloride (DAPI, 1:10,000, Sigma) and subsequent mounting and embedding under cover glasses using fluorescence mounting medium (Dako, Hamburg, Germany).

In human post-mortem brain tissue, tissue specific autofluorescence was quenched using Sudan black dissolved in 70% ethanol at 60 °C for 30 s prior to mounting under cover glasses.

Electron microscopy

For electron microscopy, animals were transcardially perfused with PBS followed by a fixative containing PBS with 4% PFA (Serva) and 0,1% glutaraldehyde (Serva). Next, serial sections of 50 μm thickness were cut using a vibrating microtome (Leica Microsystems, Wetzlar, Germany), collected in PBS, and blocked with 5% NGS in Tris-buffered saline (TBS). Sections were incubated over night at 4 °C with Iba-1 primary antibody (1:200; Wako). After rinsing in TBS samples were incubated with a biotinylated anti-rabbit secondary antibody (1:250; Sigma-Aldrich, St. Louis, MO, USA; B8895). Sections were then rinsed in TBS and incubated with ExtrAvidin Peroxidase (1:100, Sigma-Aldrich) for 1 h followed by peroxidase-dependent visualization with 3,3' Diaminobenzidine (DAB, Sigma-Aldrich) in TBS. Sections were further stained with 0.5% osmium tetroxide (EMS, Hatfield, PA, USA), dehydrated and further stained in 1% uranyl acetate (Serva) followed by final dehydration and incubation in Durcupan (Sigma-Aldrich). The sections were embedded in between coated microscope slides and coverslips and polymerized at 56 °C for 48 h. Regions of interest were located by light microscopy, marked and transferred on blocks of resin to prepare ultra-thin serial sections of 55 nm thickness using an ultra-microtome (Leica Microsystems) and transferred on formvar-coated copper grids. Finally, samples were stained with lead citrate. Analysis was performed with a Zeiss SIGMA electron microscope (Zeiss NTS, Oberkochen, Germany).

Quantification and statistical analysis

Fluorescence microscopy- based analyses were performed using a confocal laser scanning microscope (Olympus FluoView FV 1000, Olympus, Hamburg, Germany). Arteries, capillaries and veins were differentiated by diameter and presence or absence of α -SMA immunoreactivity (Hanske et al. 2016; Hawkes et al. 2011; Krueger et al. 2017). In brief, arteries were identified by their expression of α -SMA and a diameter larger than 10 μm , whereas vessels with a diameter larger than 10 μm and a lacking immunoreactivity for α -SMA were considered as post-capillary venules or veins. As the vascular wall of post-capillary venules and veins is regularly lacking a continuous layer of vascular smooth muscle cells within the CNS, they were not further differentiated for the intended analyses (Edvinsson et al. 1983; Hanske et al. 2016). Capillaries were identified by a diameter smaller than 10 μm . For each type of vessel, per mouse, at least 1000 μm of vascular length were analysed. Contacts of microglial processes with the glia limitans were counted using ImageJ software (NIH, USA). Thereby, either the average number of contacts per mm of vascular length was calculated, or the average number of contacts per mm^2

of basement membrane surface to normalize for differing vascular calibers between capillaries and arteries or veins. Acquisition settings were kept constant for each of the performed analyses. To capture minor peripheral microglial processes, gray values of the brighter cell bodies regularly appear saturated. Statistical analysis was performed with Prism 5 (GraphPad Software, La Jolla, CA, USA). For multiple comparisons, the one-way ANOVA analysis followed by Bonferroni's Multiple Comparison was applied, whereas the Mann–Whitney test was used to check for statistical significance between two groups. In general, a $p < 0.05$ was considered statistically significant.

Results

Electron microscopy reveals a microglial participation in the formation of the glia limitans of arteries, capillaries and veins

To determine whether microglial processes contribute to the formation of the glia limitans around arteries, capillaries and veins, we performed electron microscopy in brain sections of wild-type C57Bl/6 mice. For clear-cut identification of microglial cells, vibratome sections determined for electron microscopy analyses were immunolabeled for the microglia marker Iba-1 prior to the embedding in resin and prior to preparation of ultra-thin sections. While capillaries can easily be distinguished from larger blood vessels by a small diameter of less than 10 μm with only one or two endothelial cells contributing to the luminal circumference, vessels of a larger diameter are regarded as arteries or veins, depending on the presence or absence of vascular smooth muscle cells. While arteries regularly exhibit a continuous layer of smooth muscle cells, even larger cerebral veins do not show a tunica media consisting of smooth muscle cells (Hawkes et al. 2011; Krueger et al. 2017). Of note, direct microglial contacts to the glial basement membrane were regularly observed throughout the cerebral vascular tree, including arteries, capillaries and veins (Fig. 1). Thereby, in all the mice analyzed ($n = 5$), microglial contacts were not only observed for cell bodies, but for microglial endfeet as well (Fig. 1).

Capillaries show the highest density of microglial contacts in the glia limitans compared to arteries and veins

To quantitatively address differences in the distribution of microglial contacts to the glia limitans in different vessel types, we applied confocal laser scanning microscopy in sections obtained from CX3CR1^{+/GFP} mice, which offer the advantage of a very bright GFP signal, even in the smallest

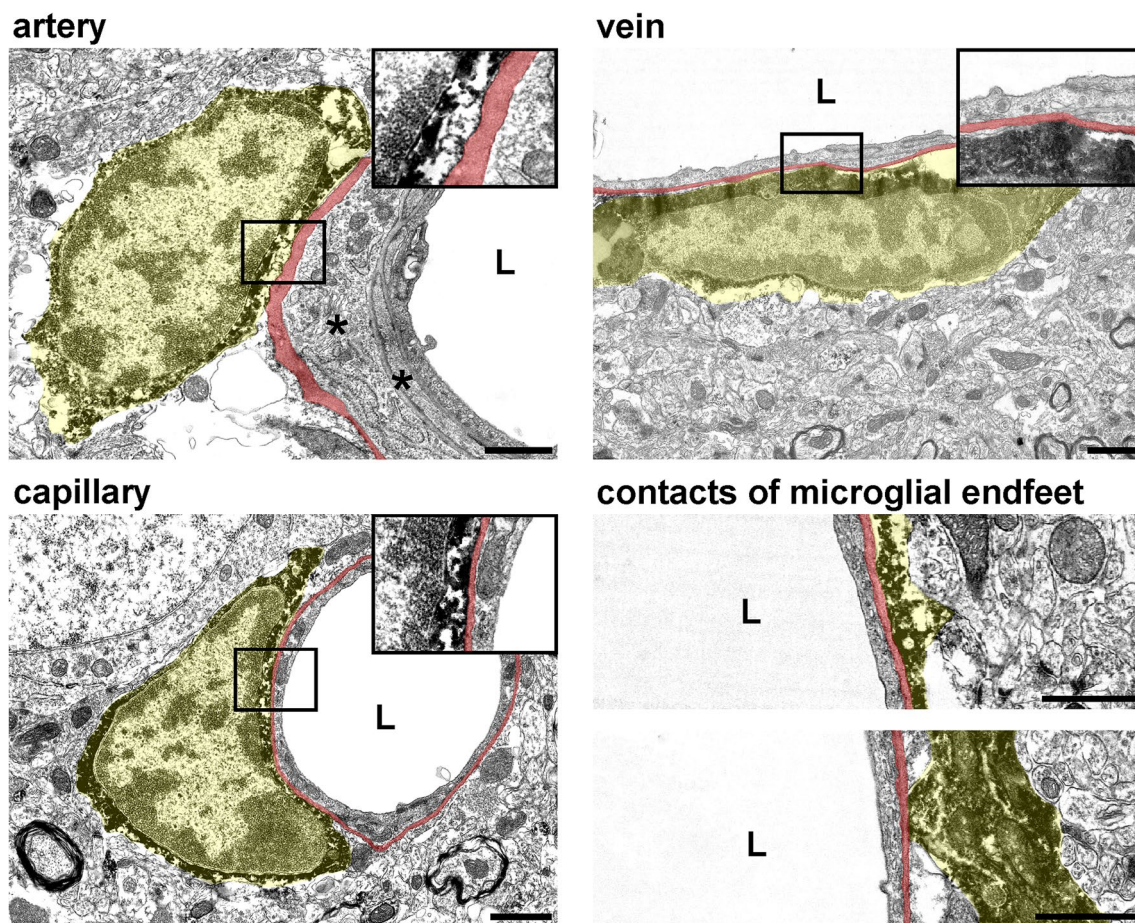


Fig. 1 Immune electron microscopy demonstrates the direct contact of Iba-1-labeled microglia (transparently highlighted in yellow) towards the glial basement membrane (transparently highlighted in red) in the arterial, capillary and venous segments of the vascular tree. Of note, microglial contacts not only comprise the cell bodies,

but also microglial endfeet as individual cellular processes. Insets show representative contact sites at higher magnification. Here, the electron-dense DAB grains of the Iba-1 immunolabeling can be easily recognized. L = vascular lumen, asterisk = arterial smooth muscle cell, Scale bars: 1 μ m

microglial endfeet (Jung et al. 2000). Here, a polyclonal pan-laminin antibody was used to delineate vascular and glia limitans-related basement membranes (Sixt et al. 2001). For the intended analyses, capillary vessels can easily be identified by a diameter smaller than 10 μ m, whereas arteries can be distinguished by their α -SMA immunoreactivity, which is lacking in post-capillary venules and veins (Hawkes et al. 2011; Krueger et al. 2017). Since CX3CR1^{+GFP} mice do not allow the differentiation of intrinsic microglia from peripheral or other CNS macrophages residing in perivascular spaces, our analyses were confined to parenchymal GFP-positive cells and processes. Here, double immunofluorescence labeling of the specific microglial markers TMEM119 and P2YR12 confirmed that the parenchymal CX3CR1^{+GFP}-positive population is also positive for both microglia-specific markers (Supplementary Fig. 1). Importantly, a subpopulation of the CX3CR1^{+GFP}-positive microglia also expressed the complement receptor CD11c (Supplementary Fig. 2),

which is also expressed on dendritic cells (Geissmann et al. 2010). Next, parenchymal CX3CR1^{+GFP}-positive microglial contacts to laminin-positive glial basement membranes were counted using high power magnification in confocal single planes, whereas GFP-positive cells within perivascular spaces were not included. In detail, the analyses comprised at least 1000 μ m of vascular length for each type of vessel in each of the analyzed animals (Fig. 2a). Thereby, the lowest numbers of microglial contacts to the glia limitans per mm of vascular length were observed around arteries, while a significantly higher microglial contribution ($p < 0.001$, $n = 6$, one-way ANOVA followed by Bonferroni's test for multiple comparison) was observed around capillaries and veins (Fig. 2b). In consideration of the larger diameters of arteries and veins with a consequentially greater outer vascular surface, we further analyzed the density of microglial contacts per area (mm^2) to normalize for differing diameters and the differing areas of vascular surface covered by the

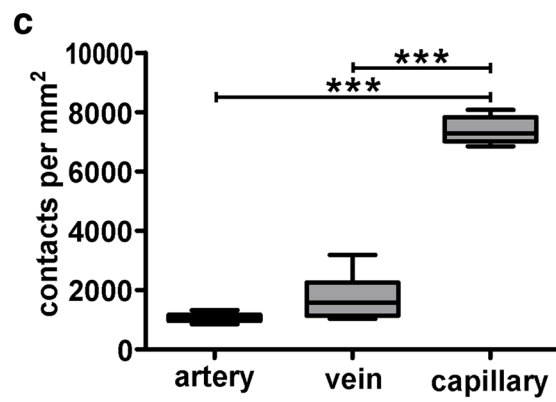
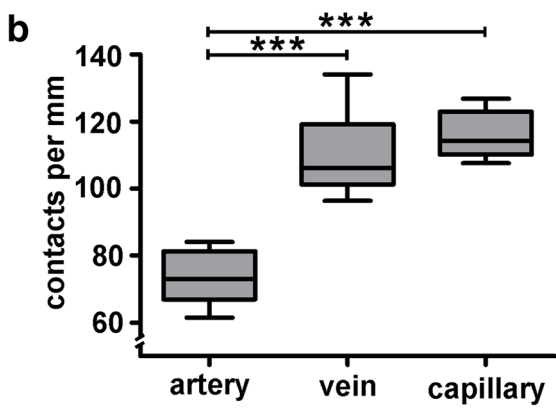
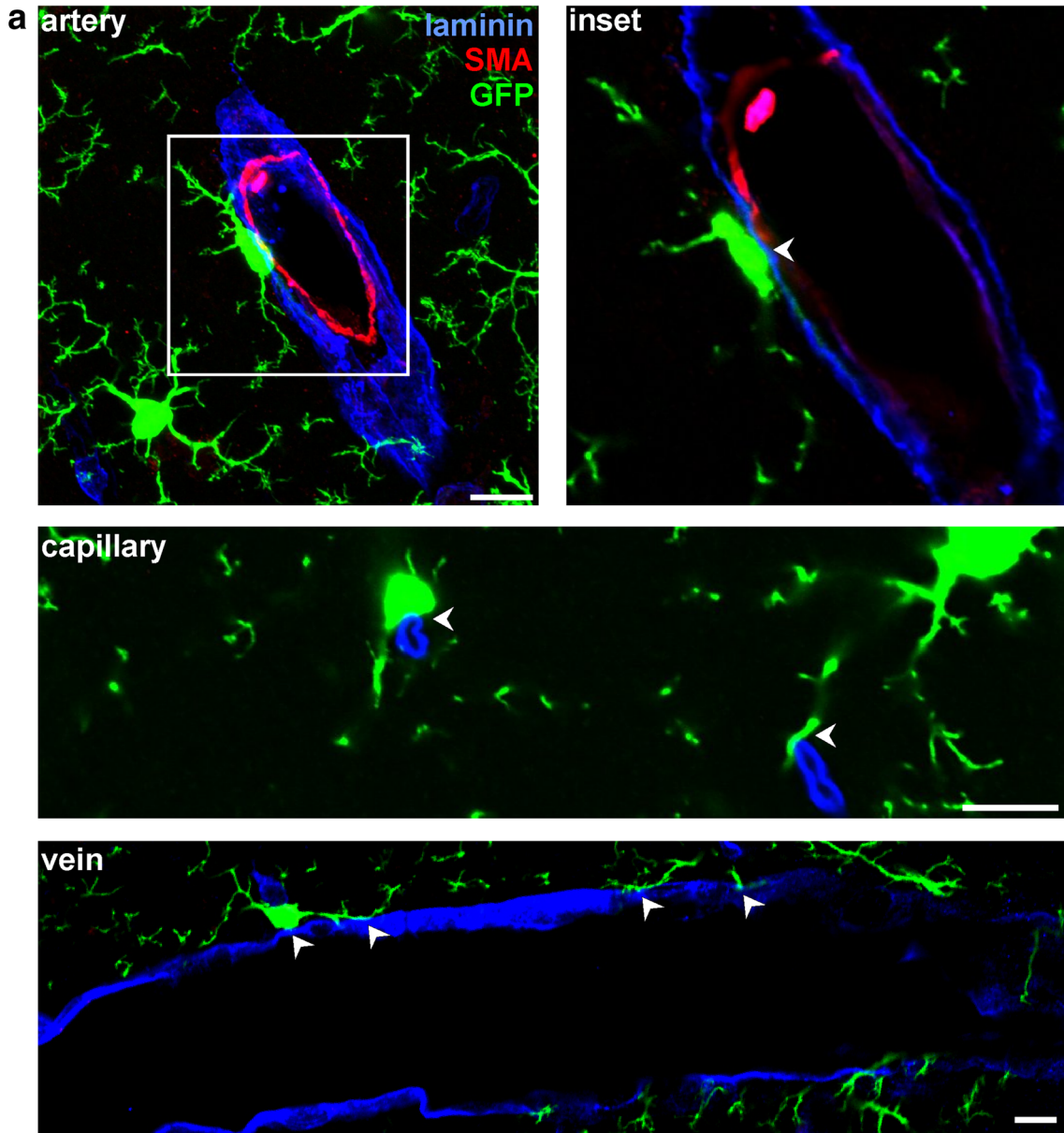


Fig. 2 a Confocal laser scanning microscopy of CX3CR1^{+/GFP} mice illustrates contacts of GFP-positive microglia to the glial basement membrane around arterial, capillary and venous vessels. Vascular and glial basement membranes are demarked by anti-laminin immunolabeling, whereas SMA immunolabeling is used to identify arterial vascular smooth muscle cells. Upper panel, left: Z-projection showing an arterial vessel. The inset demarks the area of the confocal single plane image demonstrating the microglial contact (arrow head) to the glial basement membrane. For the vein and capillary, only confocal single plane images are shown. Scale bars: 10 μm . **b** Quantification of microglial contacts per mm of vascular length ($p < 0.001$, $n = 6$, one-way ANOVA followed by Bonferroni's test for multiple comparison). **c** Analysis of the density of microglial contacts per mm^2 of vascular circumference normalizing for differences of diameter-related changes of the glial basement membrane surface ($p < 0.001$, $n = 6$, one-way ANOVA followed by Bonferroni's test for multiple comparison)

glial basement membrane, respectively. Importantly, this approach clearly demonstrates a four times higher density of microglial endfeet participating in the glia limitans at the capillary level compared to arteries and veins, which robustly reached statistical significance ($p < 0.001$, $n = 6$, one-way ANOVA followed by Bonferroni's test for multiple comparison) (Fig. 2c).

Microglia participate in the formation of the glia limitans in human post-mortem brain tissue

To investigate the contribution of microglia in the formation of the glia limitans in humans, we extended our analyses to human post-mortem brain tissue without evidence for neuropathological disorders. Importantly, the visualization of human glial and vascular basement membranes with available antibodies in our hands proved to work much better using antibodies directed against collagen-IV compared to laminin. Therefore, we applied triple immunofluorescence labeling of collagen-IV to demark basement membranes, Iba-1 to identify microglial cells and their endfeet as well as α -SMA to discriminate between arteries and veins. Of note and in line with the analyzed mouse tissue, microglial contacts to the glial basement membrane were observed around arteries, capillaries and veins (Fig. 3). However, as the human tissue was limited, a detailed quantitative analysis was not performed.

Distribution of microglial contacts remains unaltered, while contact size of individual endfeet is increased around arteries and veins under EAE conditions

Since extravasation of leukocytes under neuroinflammatory conditions is known to preferentially occur in post-capillary venules (Agrawal et al. 2006; Bechmann et al. 2007), we hypothesized that the density of microglial contacts is likely to increase in the setting of neuroinflammation.

To investigate alterations in the distribution of microglial contacts to the glial basement membrane under inflammatory conditions, we applied the model of EAE in CX3CR1^{CreERT2}:R26-Tomato reporter mice. Importantly, this model offers the advantage to discriminate resident microglia from infiltrating blood-borne leukocytes, since the reporter tomato is only expressed in resident microglia and CNS-associated macrophages such as perivascular macrophages (Goldmann et al. 2016). The latter can easily be excluded from the analysis by their localization on the vascular surface of the glial basement membrane. Noteworthy, although the microglial CX3CR1-related tomato expression was found to be increased in the setting of acute and chronic EAE (Fig. 4), we did not observe a difference in the density of microglial basement membrane contacts between the chronic, acute phase and non-immunized animals, respectively (Fig. 5). In line with the findings obtained from the CX3CR1^{+/GFP} mice described above, the highest density of microglial endfeet contacting the glia limitans was observed in the capillary segment (Fig. 5a). However, as individual microglial endfeet in the setting of EAE appeared less slender and rather blunt, we next measured the average contact length per endfeet in the setting of EAE compared to non-immunized animals. Here, the general contact length appeared to be increased in the setting of EAE (Fig. 5b), reaching statistical significance in the arterial and venous segments compared to non-immunized animals ($p < 0.01$, one-way ANOVA followed by Bonferroni's test for multiple comparison), while a robust trend towards an increased contact length was observed at the capillary level (Fig. 5b). To rule out whether there are differences between post-capillary venules showing infiltrates of leukocytes and post-capillary venules lacking these infiltrates, we further grouped and compared the venous vessels for their presence EAE-related infiltrates. Here, the direct comparison did neither reveal statistically significant differences for the distribution nor in the individual contact length of microglial endfeet (Supplementary Fig. 3).

No differences were observed for the average microglial contact length when comparing the acute and chronic phase EAE animals (not shown).

MHC-II expression is up-regulated in microglia of the glia limitans irrespective of the presence of perivascular infiltrates under inflammatory conditions

In contrast to peripheral and other brain macrophages, microglia are lacking MHC-II expression under physiological conditions (Immig et al. 2015), whereas their capacity of an MHC-II/CD86-dependent antigen presentation has been shown under experimental conditions (Bechmann et al. 2001; Ebner et al. 2013; Schettters et al. 2017). Therefore, we further analyzed

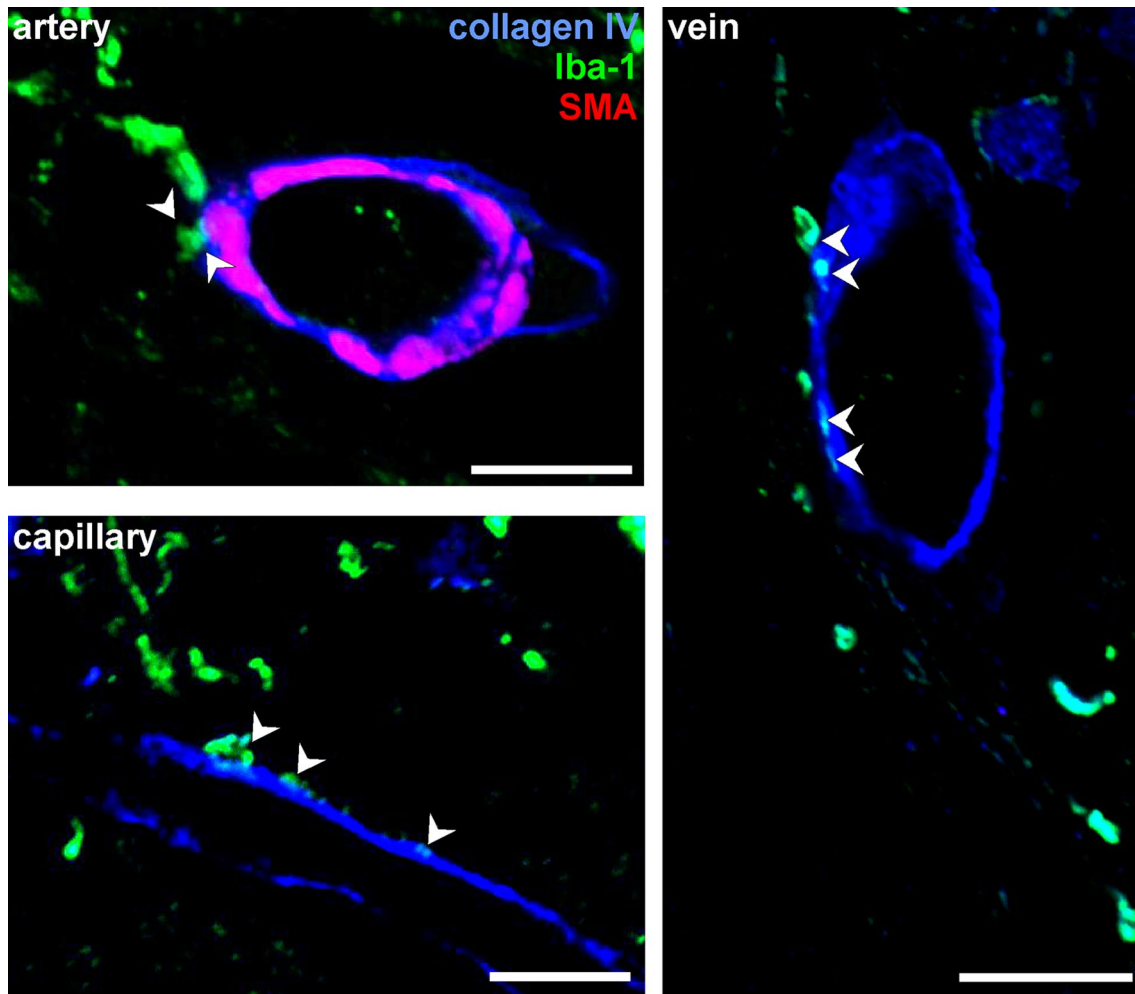


Fig. 3 Triple immunofluorescence labeling demonstrates the presence of microglial contacts (arrow heads) to the glial basement membrane in human post-mortem brain tissue. Microglia are demarked by Iba-1

immunolabeling, whereas collagen-IV is used to identify vascular and glial basement membranes. Arteries are identified by α -SMA-positive vascular smooth muscle cells. Scale bars: 10 μ m

whether an upregulation of MHC-II in the setting of EAE also involves microglia of the glia limitans. While non-immunized animals are lacking a microglial expression of MHC-II, the latter is only observed for perivascular macrophages (Fig. 6). In contrast, acute and chronic phase EAE tissue shows a dramatic increase of MHC-II expression in parenchymal microglia, which also involves microglia participating in the formation of the glia limitans. Of note, this expression does not depend on the presence of perivascular infiltrates of leukocytes around veins or post-capillary venules but is also observed at the level of capillaries (Fig. 6).

Discussion

Although microglia are lacking MHC-II expression under physiological conditions (Immig et al. 2015), their capacity of an MHC-II/CD86 dependent antigen presentation

has been demonstrated upon challenge under experimental conditions (Ebner et al. 2013; Schetters et al. 2017). In this context, their potential role as gatekeepers for infiltrating T cells has been discussed (Engelhardt et al. 2016). It is, therefore, important to note that microglia are reported to contribute to the formation of the perivascular glia limitans under inflammatory conditions and in predilection areas of multiple sclerosis (Lassmann et al. 1991; Proding et al. 2011), which renders them ideally positioned to control or respond to leukocyte infiltration. However, the NVU represents a highly specialized structure which not only functionally, but also morphologically differs when comparing arterial, capillary and venous segments of the vascular tree. Furthermore, leukocyte infiltrations are predominantly found around post-capillary venules being linked to the presence of certain laminin isoforms in vascular basement membranes (Sixt et al. 2001). Therefore, the present study was aimed to investigate the distribution of the microglial participation

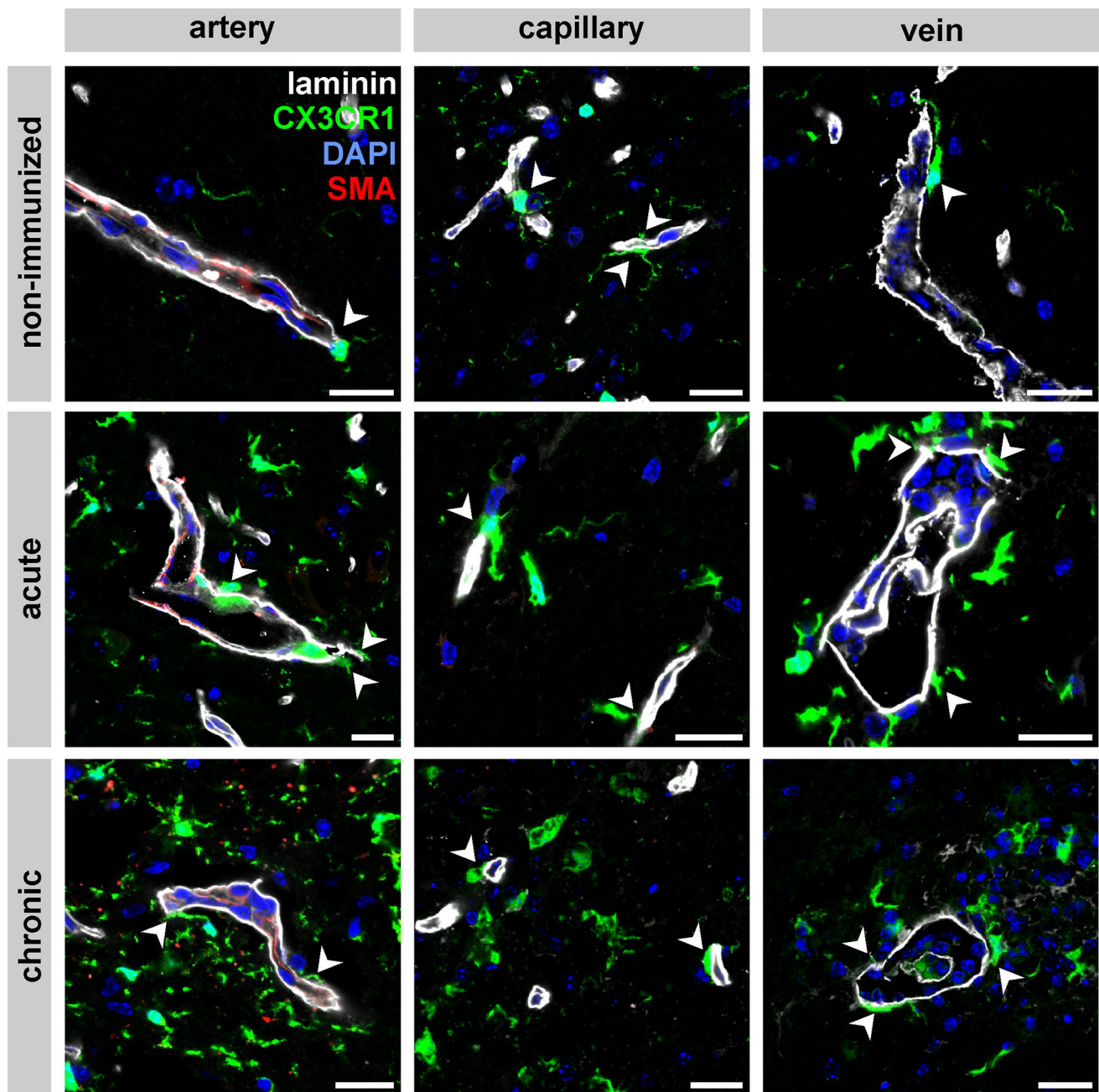


Fig. 4 Multiple fluorescence labeling of non-immunized, acute and chronic stage EAE CX3CR1^{CreERT2}.R26-Tomato reporter mice illustrating the contribution of microglia (green) to the glia limitans (arrow heads). The vascular and glial basement membranes are outlined by anti-laminin immunolabeling. SMA immunolabeling of vascular smooth muscle cells is used to identify arterial vessels. While

microglial contacts to the glial basement membrane are regularly observed throughout arterial, capillary and venous vessels in non-immunized and EAE animals, individual microglial cells as well as their endfeet contacting the basement membrane appear less slender and rather blunt in EAE animals. Nuclei are visualized with DAPI. Scale bars: 20 μ m

in the glia limitans throughout the vascular tree in arterial vessels, capillaries and veins.

For this purpose, immunolabeling of the microglial marker Iba-1 in combination with DAB was applied on PFA/GA-fixed mouse brain sections. Here, microglia were found to regularly participate in the formation of the glia limitans

around arteries, capillaries and veins. These contacts were not only found for microglial cell bodies, but also for smaller processes, all of which directly contact the glial basement membrane. Although Iba-1 immunolabeling alone does not allow a differentiation between parenchymal microglia and macrophages residing in perivascular spaces (Goldmann

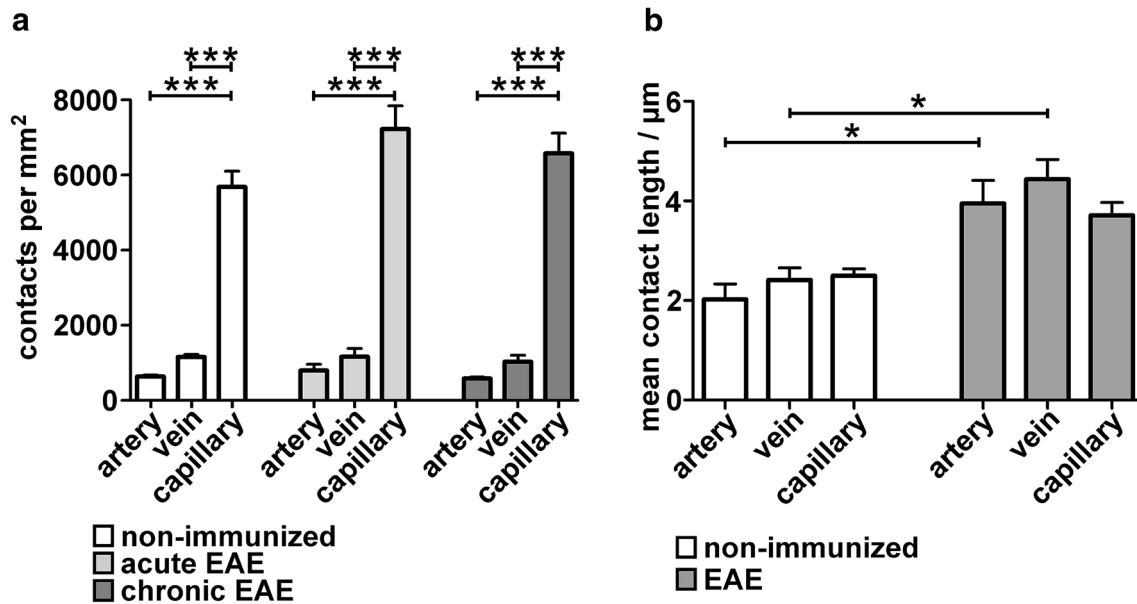


Fig. 5 **a** Density of microglial endfeet contacting the glial basement membrane of arteries, capillaries and veins in non-immunized, acute and chronic stage EAE animals ($p < 0.001$, one-way ANOVA followed by Bonferroni's test for multiple comparison, non-immunized: $n = 3$, acute EAE: $n = 6$, chronic EAE: $n = 5$). **b** Analysis of the mean

contact length of individual microglial endfeet to the glial basement membrane in non-immunized and EAE animals ($p < 0.01$, one-way ANOVA followed by Bonferroni's test for multiple comparison, non-immunized: $n = 3$, EAE: $n = 11$)

et al. 2016), microglia can easily be distinguished by their parenchymal localization, whereas Iba-1 immunopositive macrophages residing in perivascular spaces were not included in the present analysis. After confirming the direct microglial contact to the astroglial basement membrane, we next tried to address the density of microglial contacts to the glia limitans comparing arteries, capillaries and veins. For this purpose, we applied confocal laser scanning microscopy in sections obtained from CX3CR1^{+GFP} mice (Jung et al. 2000). Using this model, microglia were identified by their CX3CR1-dependent GFP expression, while laminin and collagen-IV immunolabeling was used to identify vessels and the glial basement membranes as well (Sixt et al. 2001; Hawkes et al. 2011; Krueger et al. 2017). Of note, this approach not only allows to label each type of vessel, irrespective of the position in the vascular tree, but also in the absence of additional methods for antigen retrieval (Sixt et al. 2001; Hawkes et al. 2011; Krueger et al. 2017). Here, capillary vessels can easily be identified by a diameter smaller than 10 µm, whereas arteries can be distinguished by their immunoreactivity for α-SMA, which is lacking in post-capillary venules or larger veins (Hawkes et al. 2011; Krueger et al. 2017). Importantly, after normalizing for different vascular calibers, the highest density of microglial endfeet contacting the astroglial basement membrane is demonstrated for capillaries. Since capillaries are shown to predominantly contribute to blood-brain barrier breakdown in the setting of experimental stroke (Krueger et al. 2017),

it is important to note that microglia have been identified to mediate cerebrovascular permeability following ischemia (Su et al. 2017). In this setting, juxtavascular microglia contacting the vascular wall have also been hypothesized to be involved in the phagocytosis of ischemia-affected endothelial cells (Jolivel et al. 2015), although the authors leave open the question whether or not microglia are capable to overcome the vascular basement membranes.

In the setting of neuroinflammation, post-capillary venules are regarded as preferential sites of leukocyte infiltration (Agrawal et al. 2006). Here, leukocyte transmigration across the glia limitans is known to depend on a matrix-metalloproteinase-mediated cleavage of dystroglycan to detach astrocytic endfeet from the parenchymal basement membrane (Agrawal et al. 2006; Hännöcks et al. 2017).

Therefore, we further investigated the distribution of microglial endfeet in the glia limitans under neuroinflammatory conditions in the setting of EAE, which represents an established animal model of multiple sclerosis (Lassmann and Bradl 2017). As infiltrates of blood-borne leukocytes are known to express typical microglial markers, we took advantage of the CX3CR1^{CreERT2}:R26-Tomato reporter mouse model (Goldmann et al. 2016). Thus, resident CX3CR1+ microglia can be distinguished from extravasated myeloid cells, which was a prerequisite for the intended analyses. Importantly, in both CX3CR1-related reporter mouse models, CX3CR1-positive cells were not only found to co-express the specific microglial markers TMEM119

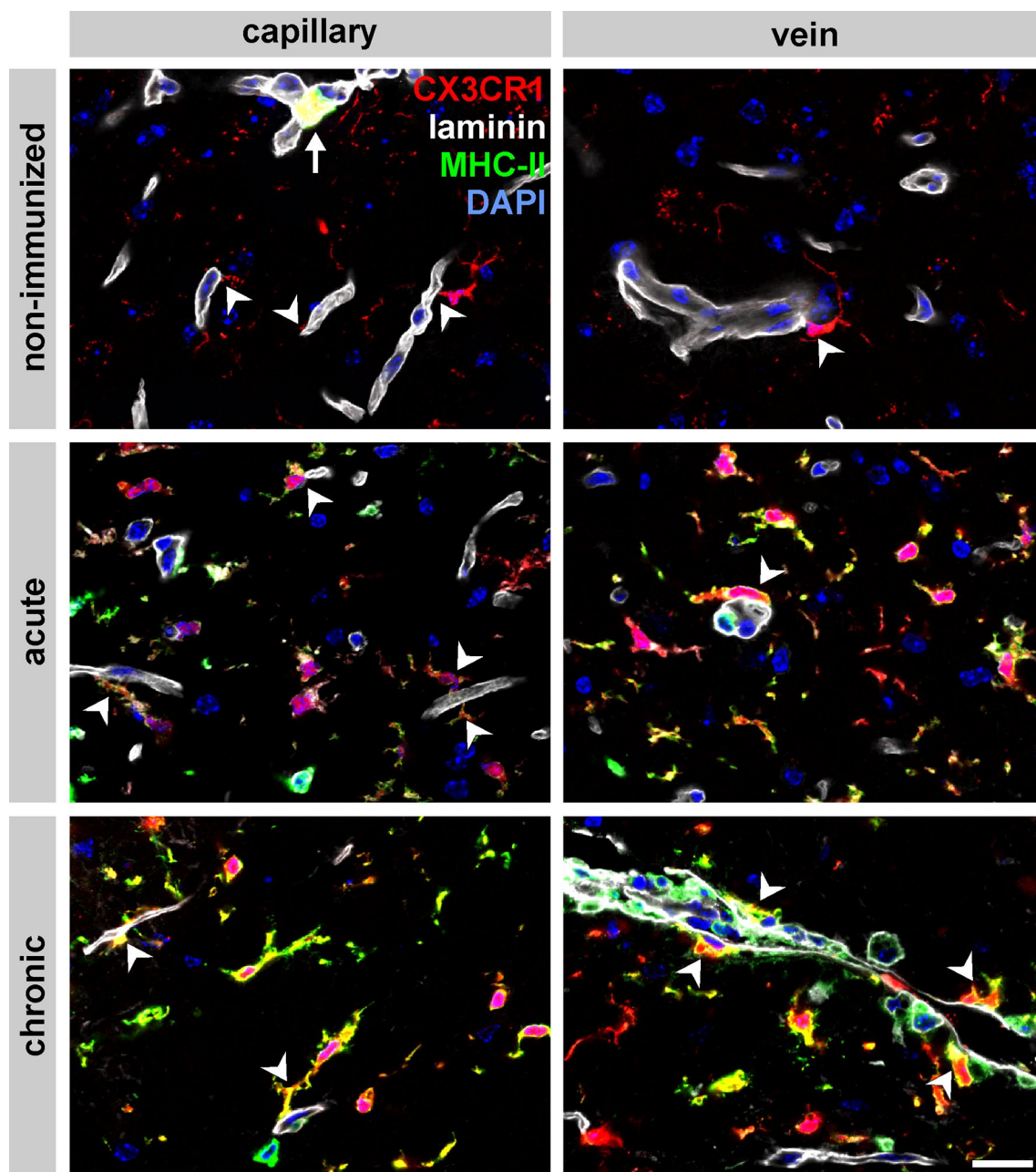


Fig. 6 Multiple immunofluorescence labeling of non-immunized, acute and chronic stage EAE CX3CR1^{CreERT2}:R26-Tomato reporter mice illustrating the contribution microglia (red) to the glia limitans (arrow heads). The vascular and glial basement membranes are outlined by anti-laminin immunolabeling. In non-immunized animals, MHC-II expression is confined to perivascular macrophages (arrow), while parenchymal microglia are lacking MHC-II expression. In con-

trast, acute and chronic stage EAE animals show an upregulation of MHC-II in parenchymal microglia as well as in microglia contacting the glial basement membrane (arrow heads). Of note, MHC-II expression is not confined to microglia around veins with perivascular infiltrates but is also observed at the level of capillaries. Nuclei are visualized with DAPI. Scale bar: 20 μ m

and P2YR12 (Bennett et al. 2016; Mildner et al. 2017). Moreover, a subpopulation of CX3CR1- positive microglia also expressed the complement receptor CD11c, which is also expressed on dendritic cells of various organs (Geissmann et al. 2010; Immig et al. 2015). Although we initially hypothesized that the density of microglial endfeet within

the glia limitans would be increased under neuroinflammatory conditions, especially at the level of post-capillary venules, the relative density remained unaltered when compared to non-immunized animals. Again, the highest density was observed around capillary vessels. Of note, especially at the level of post-capillary venules an increase of the microglial

endfeet density was neither detectable when comparing EAE animals to the non-immunized controls, nor when comparing acute and chronic phase animals. However, in direct comparison to the non-immunized animals microglial processes appeared to be thicker under EAE conditions. Analysis of the mean length of individual microglial contacts to the basement membrane revealed that the individual contact size was increased throughout arteries, capillaries and veins, with the most pronounced increase at the level of veins showing peri- and juxtavascular infiltrates of leukocytes. Of note, microglia have been shown to represent a source of matrix metalloproteinases thereby potentially promoting the infiltration of leukocytes into the adjacent neuropil. However, in the setting of EAE this expression is specifically downregulated in microglia, which potentially reflects their transition from a rather resting to an activated state (Toft-Hansen et al. 2004).

Since microglia as gatekeepers under neuroinflammatory conditions (Engelhardt et al. 2016) would be ideally positioned at the glia limitans of post-capillary venules and veins, we further explored their capacity of MHC-II expression (Ebner et al. 2013; Schettters et al. 2017) in the setting of EAE to investigate differences between juxtavascular microglia around capillaries and post-capillary venules. Of note, the increase of microglial MHC-II expression did not only involve parenchymal microglia, but also microglia contributing to the glia limitans. Here, MHC-II-positive microglia were not only present around post-capillary venules and veins, but also at the level of capillaries showing no infiltrates of leukocytes at all. In this context, it is important to note that microglial processes have been described to extend through the vascular wall into the vascular lumen, which would allow a direct communication with the peripheral immune system (Barkauskas et al. 2013). As this feature would have multiple implications for leukocyte recruitment, we extensively searched for microglial endfeet reaching into perivascular spaces or the vascular lumen in serial sections for electron microscopy. However, we did not find a single microglial process penetrating the glial basement membrane. Given that the average thickness of the glial basement membrane is only measuring 20 nm (Thomsen et al. 2017), these structures are clearly below the diffraction barrier and even below the resolution limit of super resolution microscopy (Hell and Wichmann 1994). Therefore, confocal and two-photon images may offer the false impression that microglial endfeet penetrate the glia limitans or even the vascular wall, especially in tangentially sectioned vessels.

Although the present study tends to be rather descriptive in its design and the data presented, we here for the first time systematically investigate the microglial contribution to the glia limitans along the vascular tree under physiological conditions and in the setting of neuroinflammation, as well as in human brain tissue. Since several neuropathologies

including stroke, Alzheimer's disease, cancer, neurodegenerative diseases and neuroinflammation (Liebner et al. 2018; Rodrigues et al. 2012; Sweeney et al. 2018) share the feature of a vascular affection, the presented findings and analyses may help to investigate the role of microglia within the NVU in different neuropathologies.

Funding This work was supported by Deutsche Forschungsgemeinschaft (SFB Grant 1052 'Obesity mechanisms') to IB.

Compliance with ethical standards

Conflicts of interest The authors declare that there is no conflict of interest.

Ethical approval All procedures performed in studies involving human tissue were in accordance with the ethical standards of the institutional and/or national research committee and with the 1964 Helsinki Declaration and its later amendments or comparable ethical standards.

Research involving human and/or animal participants All applicable international, national, and/or institutional guidelines for the care and use of animals were followed.

References

- Agrawal S, Anderson P, Durbeej M, van Rooijen N, Ivars F, Opendaker G, Sorokin LM (2006) Dystroglycan is selectively cleaved at the parenchymal basement membrane at sites of leukocyte extravasation in experimental autoimmune encephalomyelitis. *J Exp Med* 203:1007–1019. <https://doi.org/10.1084/jem.20051342>
- Ajami B, Bennett JL, Krieger C, Tetzlaff W, Rossi FMV (2007) Local self-renewal can sustain CNS microglia maintenance and function throughout adult life. *Nat Neurosci* 10:1538–1543. <https://doi.org/10.1038/nn2014>
- Alliot F, Godin I, Pessac B (1999) Microglia derive from progenitors, originating from the yolk sac, and which proliferate in the brain. *Dev Brain Res* 117:145–152. [https://doi.org/10.1016/S0165-3806\(99\)00113-3](https://doi.org/10.1016/S0165-3806(99)00113-3)
- Askew K, Li K, Olmos-Alonso A, Garcia-Moreno F, Liang Y, Richardson P, Tipton T, Chapman MA, Riecken K, Beccari S, Sierra A, Molnár Z, Cragg MS, Garaschuk O, Perry VH, Gomez-Nicola D (2017) Coupled proliferation and apoptosis maintain the rapid turnover of microglia in the adult brain. *Cell Rep* 18:391–405. <https://doi.org/10.1016/j.celrep.2016.12.041>
- Barkauskas DS, Evans TA, Myers J, Petrosiute A, Silver J, Huang AY (2013) Extravascular CX3CR1⁺ cells extend intravascular dendritic processes into intact central nervous system vessel lumen. *Microsc Microanal* 19:778–790. <https://doi.org/10.1017/S1431927613000482>
- Bechmann I, Kwizdzinski E, Kovac AD, Simbürger E, Horvath T, Gimsa U, Dirnagl U, Priller J, Nitsch R (2001) Turnover of rat brain perivascular cells. *Exp Neurol* 168:242–249. <https://doi.org/10.1006/exnr.2000.7618>
- Bechmann I, Goldmann J, Kovac AD, Kwizdzinski E, Simbürger E, Naftolin F, Dirnagl U, Nitsch R, Priller J (2005) Circulating monocytic cells infiltrate layers of anterograde axonal degeneration where they transform into microglia. *FASEB J* 19:647–649. <https://doi.org/10.1096/fj.04-2599fje>

- Bechmann I, Galea I, Perry VH (2007) What is the blood–brain barrier (not)? *Trends Immunol* 28:5–11. <https://doi.org/10.1016/j.it.2006.11.007>
- Bennett ML, Bennett FC, Liddel SA, Ajami B, Zamanian JL, Fernhoff NB, Mulinyawe SB, Bohlen CJ, Adil A, Tucker A, Weissman IL, Chang EF, Li G, Grant GA, Hayden Gephart MG, Barres BA (2016) New tools for studying microglia in the mouse and human CNS. *Proc Natl Acad Sci USA* 113:E1738–E1746. <https://doi.org/10.1073/pnas.1525528113>
- Colonna M, Butovsky O (2017) Microglia function in the central nervous system during health and neurodegeneration. *Annu Rev Immunol* 35:441–468. <https://doi.org/10.1146/annurev-immunol-051116-052358>
- Dyrna F, Hanske S, Krueger M, Bechmann I (2013) The blood–brain barrier. *J Neuroimmune Pharmacol* 8:763–773. <https://doi.org/10.1007/s11481-013-9473-5>
- Ebner F, Brandt C, Thiele P, Richter D, Schliesser U, Siffrin V, Schueler J, Stubbe T, Ellinghaus A, Meisel C, Sawitzki B, Nitsch R (2013) Microglial activation milieu controls regulatory T cell responses. *J Immunol* 191:5594–5602. <https://doi.org/10.4049/jimmunol.1203331>
- Edvinsson L, Högestätt ED, Uddman R, Auer LM (1983) Cerebral veins: fluorescence histochemistry, electron microscopy, and in vitro reactivity. *J Cereb Blood Flow Metab* 3(2):226–230
- Engelhardt B, Carare RO, Bechmann I, Flugel A, Laman JD, Weller RO (2016) Vascular, glial, and lymphatic immune gateways of the central nervous system. *Acta Neuropathol* 132:317–338. <https://doi.org/10.1007/s00401-016-1606-5>
- Geissmann F, Gordon S, Hume DA, Mowat AM, Randolph GJ (2010) Unravelling mononuclear phagocyte heterogeneity. *Nat Rev Immunol* 10:453–460. <https://doi.org/10.1038/nri2784>
- Gertig U, Hanisch U-K (2014) Microglial diversity by responses and responders. *Front Cell Neurosci* 8:101. <https://doi.org/10.3389/fncel.2014.00101>
- Ginhoux F, Greter M, Leboeuf M, Nandi S, See P, Gokhan S, Mehler MF, Conway SJ, Ng LG, Stanley ER, Samokhvalov IM, Merad M (2010) Fate mapping analysis reveals that adult microglia derive from primitive macrophages. *Science* 330:841–845. <https://doi.org/10.1126/science.1194637>
- Goldmann T, Wieghofer P, Müller PF, Wolf Y, Varol D, Yona S, Brendecke SM, Kierdorf K, Staszewski O, Datta M, Luedde T, Heikenwalder M, Jung S, Prinz M (2013) A new type of microglia gene targeting shows TAK1 to be pivotal in CNS autoimmune inflammation. *Nat Neurosci* 16:1618–1626. <https://doi.org/10.1038/nn.3531>
- Goldmann T, Wieghofer P, Jordao MJC, Prutek F, Hagemeyer N, Frenzel K, Amann L, Staszewski O, Kierdorf K, Krueger M, Locatelli G, Hochgerner H, Zeiser R, Epelman S, Geissmann F, Priller J, Rossi FMV, Bechmann I, Kerschensteiner M, Linnarsson S, Jung S, Prinz M (2016) Origin, fate and dynamics of macrophages at central nervous system interfaces. *Nat Immunol* 17:797–805. <https://doi.org/10.1038/ni.3423>
- Hannocks M-J, Zhang X, Gerwien H, Chashchina A, Burmeister M, Korpos E, Song J, Sorokin L (2017) The gelatinases, MMP-2 and MMP-9, as fine tuners of neuroinflammatory processes. *Matrix Biol*. <https://doi.org/10.1016/j.matbio.2017.11.007>
- Hanske S, Dyrna F, Bechmann I, Krueger M (2016) Different segments of the cerebral vasculature reveal specific endothelial specifications, while tight junction proteins appear equally distributed. *Brain Struct Funct*. <https://doi.org/10.1007/s00429-016-1267-0>
- Hawkes CA, Härtig W, Kacza J, Schliebs R, Weller RO, Nicoll JA, Carare RO (2011) Perivascular drainage of solutes is impaired in the ageing mouse brain and in the presence of cerebral amyloid angiopathy. *Acta Neuropathol* 121:431–443. <https://doi.org/10.1007/s00401-011-0801-7>
- Hefendehl JK, Neher JJ, Sühs RB, Kohsaka S, Skodras A, Jucker M (2014) Homeostatic and injury-induced microglia behavior in the aging brain. *Aging Cell* 13:60–69. <https://doi.org/10.1111/ace1.12149>
- Hell SW, Wichmann J (1994) Breaking the diffraction resolution limit by stimulated emission: Stimulated-emission-depletion fluorescence microscopy. *Opt Lett* 19:780–782
- Immig K, Gericke M, Menzel F, Merz F, Krueger M, Schiefenhover F, Losche A, Jager K, Hanisch U-K, Biber K, Bechmann I (2015) CD11c-positive cells from brain, spleen, lung, and liver exhibit site-specific immune phenotypes and plastically adapt to new environments. *Glia* 63:611–625. <https://doi.org/10.1002/glia.22771>
- Jolivel V, Bicker F, Binamé F, Ploen R, Keller S, Gollan R, Jurek B, Birkenstock J, Poisa-Beiro L, Bruttger J, Opitz V, Thal SC, Waisman A, Bäuerle T, Schäfer MK, Zipp F, Schmidt MHH (2015) Perivascular microglia promote blood vessel disintegration in the ischemic penumbra. *Acta Neuropathol* 129:279–295. <https://doi.org/10.1007/s00401-014-1372-1>
- Jung S, Aliberti J, Graemmel P, Sunshine MJ, Kreutzberg GW, Sher A, Littman DR (2000) Analysis of fractalkine receptor CX3CR1 function by targeted deletion and green fluorescent protein reporter gene insertion. *Mol Cell Biol* 20:4106–4114. <https://doi.org/10.1128/MCB.20.11.4106-4114.2000>
- Kierdorf K, Prinz M (2017) Microglia in steady state. *J Clin Invest* 127:3201–3209. <https://doi.org/10.1172/JCI90602>
- Kierdorf K, Erny D, Goldmann T, Sander V, Schulz C, Perdiguero EG, Wieghofer P, Heinrich A, Riemke P, Hölscher C, Müller DN, Luckow B, Brocker T, Debowski K, Fritz G, Opdenakker G, Diefenbach A, Biber K, Heikenwalder M, Geissmann F, Rosenbauer F, Prinz M (2013) Microglia emerge from erythromyeloid precursors via Pu.1- and Irf8-dependent pathways. *Nat Neurosci* 16:273–280. <https://doi.org/10.1038/nn.3318>
- Krueger M, Härtig W, Frydrychowicz C, Mueller WC, Reichenbach A, Bechmann I, Michalski D (2017) Stroke-induced blood–brain barrier breakdown along the vascular tree - No preferential affection of arteries in different animal models and in humans. *J Cereb Blood Flow Metab* 37:2539–2554. <https://doi.org/10.1177/0271678X16670922>
- Lassmann H, Bradl M (2017) Multiple sclerosis: Experimental models and reality. *Acta Neuropathol* 133:223–244. <https://doi.org/10.1007/s00401-016-1631-4>
- Lassmann H, Zimprich F, Vass K, Hickey WF (1991) Microglial cells are a component of the perivascular glia limitans. *J Neurosci Res* 28:236–243. <https://doi.org/10.1002/jnr.490280211>
- Lawson LJ, Perry VH, Dri P, Gordon S (1990) Heterogeneity in the distribution and morphology of microglia in the normal adult mouse brain. *Neuroscience* 39:151–170. [https://doi.org/10.1016/0306-4522\(90\)90229-W](https://doi.org/10.1016/0306-4522(90)90229-W)
- Liebner S, Dijkhuizen RM, Reiss Y, Plate KH, Agalliu D, Constantin G (2018) Functional morphology of the blood–brain barrier in health and disease. *Acta Neuropathol* 135:311–336. <https://doi.org/10.1007/s00401-018-1815-1>
- Mildner A, Schmidt H, Nitsche M, Merkler D, Hanisch U-K, Mack M, Heikenwalder M, Bruck W, Priller J, Prinz M (2007) Microglia in the adult brain arise from Ly-6ChiCCR2+ monocytes only under defined host conditions. *Nat Neurosci* 10:1544–1553. <https://doi.org/10.1038/nn2015>
- Mildner A, Huang H, Radke J, Stenzel W, Priller J (2017) P2Y12 receptor is expressed on human microglia under physiological conditions throughout development and is sensitive to neuroinflammatory diseases. *Glia* 65:375–387. <https://doi.org/10.1002/glia.23097>
- Mittelbronn M, Dietz K, Schluesener HJ, Meyermann R (2001) Local distribution of microglia in the normal adult human central

- nervous system differs by up to one order of magnitude. *Acta Neuropathol* 101:249–255
- O’Loughlin E, Madore C, Lassmann H, Butovsky O (2018) Microglial phenotypes and functions in multiple sclerosis. *Cold Spring Harb Perspect Med* 8. <https://doi.org/10.1101/cshperspect.a028993>
- Poliani PL, Wang Y, Fontana E, Robinette ML, Yamanishi Y, Gillfillan S, Colonna M (2015) TREM2 sustains microglial expansion during aging and response to demyelination. *J Clin Invest* 125:2161–2170. <https://doi.org/10.1172/JCI77983>
- Prodinger C, Bunse J, Kruger M, Schiefenhovel F, Brandt C, Laman JD, Greter M, Immig K, Heppner F, Becher B, Bechmann I (2011) CD11c-expressing cells reside in the juxtavascular parenchyma and extend processes into the glia limitans of the mouse nervous system. *Acta Neuropathol* 121:445–458. <https://doi.org/10.1007/s00401-010-0774-y>
- Rodrigues MCO, Hernandez-Ontiveros DG, Louis MK, Willing AE, Borlongan CV, Sanberg PR, Voltarelli JC, Garbuzova-Davis S (2012) Neurovascular aspects of amyotrophic lateral sclerosis. *Int Rev Neurobiol* 102:91–106. <https://doi.org/10.1016/B978-0-12-386986-9.00004-1>
- Schettler STT, Gomez-Nicola D, Garcia-Vallejo JJ, van Kooyk Y (2017) Neuroinflammation: microglia and T Cells get ready to tango. *Front Immunol* 8:1905. <https://doi.org/10.3389/fimmu.2017.01905>
- Sierra A, Gottfried-Blackmore AC, McEwen BS, Bulloch K (2007) Microglia derived from aging mice exhibit an altered inflammatory profile. *Glia* 55:412–424. <https://doi.org/10.1002/glia.20468>
- Sixt M, Engelhardt B, Pausch F., Hallmann R, Wendler O, Sorokin LM (2001) Endothelial cell laminin isoforms, laminins 8 and 10, play decisive roles in T cell recruitment across the blood–brain barrier in experimental autoimmune encephalomyelitis. *J Cell Biol* 153(5):933–946
- Streit WJ, Braak H, Xue Q-S, Bechmann I (2009) Dystrophic (senescent) rather than activated microglial cells are associated with tau pathology and likely precede neurodegeneration in Alzheimer’s disease. *Acta Neuropathol* 118:475–485. <https://doi.org/10.1007/s00401-009-0556-6>
- Su EJ, Cao C, Fredriksson L, Nilsson I, Stefanitsch C, Stevenson TK, Zhao J, Ragsdale M, Sun Y-Y, Yepes M, Kuan C-Y, Eriksson U, Strickland DK, Lawrence DA, Zhang L (2017) Microglial-mediated PDGF-CC activation increases cerebrovascular permeability during ischemic stroke. *Acta Neuropathol* 134:585–604. <https://doi.org/10.1007/s00401-017-1749-z>
- Sweeney MD, Sagare AP, Zlokovic BV (2018) Blood–brain barrier breakdown in Alzheimer disease and other neurodegenerative disorders. *Nat Rev Neurol* 14:133. <https://doi.org/10.1038/nrneuro.2017.188>
- Tay TL, Mai D, Dautzenberg J, Fernández-Klett F, Lin G, Datta M, Drougard A, Stempf T, Ardura-Fabregat A, Staszewski O, Margineanu A, Sporbert A, Steinmetz LM, Pospisilik JA, Jung S, Priller J, Grün D, Ronneberger O, Prinz M (2017) A new fate mapping system reveals context-dependent random or clonal expansion of microglia. *Nat Neurosci* 20:793–803. <https://doi.org/10.1038/nn.4547>
- Thomsen MS, Routhe LJ, Moos T (2017) The vascular basement membrane in the healthy and pathological brain. *J Cereb Blood Flow Metab* 37:3300–3317. <https://doi.org/10.1177/0271678X17722436>
- Tischer J, Krueger M, Mueller W, Staszewski O, Prinz M, Streit WJ, Bechmann I (2016) Inhomogeneous distribution of Iba-1 characterizes microglial pathology in Alzheimer’s disease. *Glia* 64:1562–1572. <https://doi.org/10.1002/glia.23024>
- Toft-Hansen H, Nuttall RK, Edwards DR, Owens T (2004) Key metalloproteinases are expressed by specific cell types in experimental autoimmune encephalomyelitis. *J Immunol* 173:5209–5218. <https://doi.org/10.4049/jimmunol.173.8.5209>
- Tremblay M-È, Zettel ML, Ison JR, Allen PD, Majewska AK (2012) Effects of aging and sensory loss on glial cells in mouse visual and auditory cortices. *Glia* 60:541–558. <https://doi.org/10.1002/glia.22287>
- Wieghofer P, Knobloch K-P, Prinz M (2015) Genetic targeting of microglia. *Glia* 63:1–22. <https://doi.org/10.1002/glia.22727>
- Wolf SA, Boddeke HWGM, Kettenmann H (2017) Microglia in Physiology and Disease. *Annu Rev Physiol* 79:619–643. <https://doi.org/10.1146/annurev-physiol-022516-034406>
- Wu C, Ivars F, Anderson P, Hallmann R, Vestweber D, Nilsson P, Robenek H, Tryggvason K, Song J, Korpos E, Loser K, Beissert S, Georges-Labouesse E, Sorokin LM (2009) Endothelial basement membrane laminin alpha5 selectively inhibits T lymphocyte extravasation into the brain. *Nat Med* 15:519–527. <https://doi.org/10.1038/nm.1957>
- Yousif LF, Di Russo J, Sorokin L (2013) Laminin isoforms in endothelial and perivascular basement membranes. *Cell Adh Migr* 7:101–110. <https://doi.org/10.4161/cam.22680>
- Zhao Z, Nelson AR, Betsholtz C, Zlokovic BV (2015) Establishment and dysfunction of the blood–brain barrier. *Cell* 163:1064–1078. <https://doi.org/10.1016/j.cell.2015.10.067>

Publisher’s Note Springer Nature remains neutral with regard to jurisdictional claims in published maps and institutional affiliations.